Supramolecular encapsulation of hexaaquocobalt(II) cations in a hydrogen-bonded framework for slow magnetic relaxation and high proton conduction

Dong Shao, *[a,c] Yue Zhou, [a] Xiaodong Yang, [a] Jing Yue, [a] Shujun Ming, [a] Xiao-Qin Wei *[b] and Zhengfang Tian [a]

[a] Hubei Key Laboratory of Processing and Application of Catalytic Materials, College of Chemistry and Chemical Engineering, Huanggang Normal University, Huanggang 438000, P. R. China

[b] b. Department of Material Science and Engineering, Shanxi Province Collaborative Innovation Center for Light Materials Modification and Application, Jinzhong University, Jinzhong, 030619, P. R. China.

[c] State Key Laboratory of Coordination Chemistry, Nanjing University, Nanjing, 210023, P. R. China.

Correspondence and requests for materials should be addressed to

Email: shaodong@nju.edu.cn

Table of Contents

EXPERIMENTAL SECTION

Physical measurements

Elemental analyses of C, H, and N were performed at an Elementar Vario MICRO analyzer. Infrared spectra were obtained in the range of 600–4000 cm^{-1} on a Bruker tensor II spectrometer. Variable-temperature powder X-ray diffraction data (PXRD) were recorded on a Bruker D8 Advance diffractometer with Cu Kα X-ray source (λ = 1.54056 Å) operated at 40 kV and 40 mA between 5 and 35° (2θ). Simulated PXRD patterns were obtained from the Mercury software. Thermal gravimetric analysis (TGA) was carried out on freshly filtered crystals using the Mettler Toledo TGA2 instrument in an insert Ar atmosphere over a temperature range of 27–700 °C with a heating rate of 10 °C/min. Low-pressure volumetric N_2 gas adsorption measurements were performed on a Quadrasorb automatic volumetric instrument. The Brunauer-Emmett-Teller (BET) method was utilized to calculate the specific surface areas. Water adsorption/desorption isotherms were measured using a BELSORP max instrument.

Proton conductivity

Proton conductivity measurements were performed using a quasi-four-electrode AC impedance technique with a Solartron 1260 impedance/gain-phase analyzer. The single crystals samples were compressed to 2.5 mm diameter, which were connected to gold wires using silver paste. The sample pellet was measured in the temperature range of 40−100 °C and in the RH range of 40−97%. The hydrated and anhydrous sample was placed in Espec Corp. SH-221 incubator for 24 h at a given temperature and relative humidity values before recording the impedance. The conductivity was calculated using the equation $\sigma = l/R_sA$, where l and A are the thickness (cm) and cross-sectional area (cm^2) of the pellet, respectively, and Rs is the bulk resistance of the sample. R_s was calculated using the Nyquist plot from impedance spectra.

Magnetic measurements

Direct current (dc) magnetic susceptibility from 2 to 300 K with applied 1000 Oe dc field were performed using a Quantum Design SQUID VSM magnetometer on the crushed single crystals sample of **1**. Alternative current (ac) magnetic susceptibility data

were collected in a zero-dc field or an applied 1000 Oe dc fields in the temperature range of 2-10 K, under an ac field of 2 Oe, oscillating at frequencies in the range of 1-1000 Hz. All magnetic data were corrected for the diamagnetic contributions of the sample holder and of core diamagnetism of the sample using Pascal's constants.

X-ray Crystallography

Single crystal X-ray diffraction data were collected on a Bruker D8 QUEST diffractometer with a PHOTON III area detector (Mo-Kα radiation, λ = 0.71073 Å, Bruker *Ius* 3.0) at different temperatures controlled by Oxford Cryosystems low-temperature device. The APEX III program was used to determine the unit cell parameters and for data collection. The data were integrated and corrected for Lorentz and polarization effects using SAINT.[S1] Absorption corrections were applied with SADABS.[S2] The structures were solved by direct methods and refined by full-matrix least-squares method on *F*2 using the SHELXTL[S3] crystallographic software package integrated in Olex 2.[S4] All the non-hydrogen atoms were refined anisotropically. Hydrogen atoms of the organic ligands were refined as riding on the corresponding non-hydrogen atoms. Additional details of the data collections and structural refinement parameters are provided in Table 1. Selected bond lengths and angles of **1** are listed in Table S1, S2. CCDC numbers 2211956-2211958 are the supplementary crystallographic data for this paper. They can be obtained freely from the Cambridge Crystallographic Data Centre via www.ccdc.cam.ac.uk/data_request/cif.

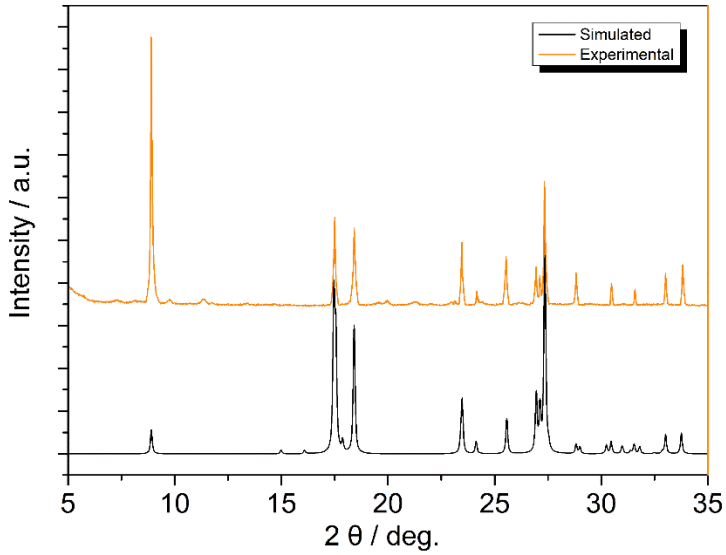

Figure S1. Comparison of the experimental PXRD pattern at room temperature of **1** with the simulated pattern from single crystal structure.

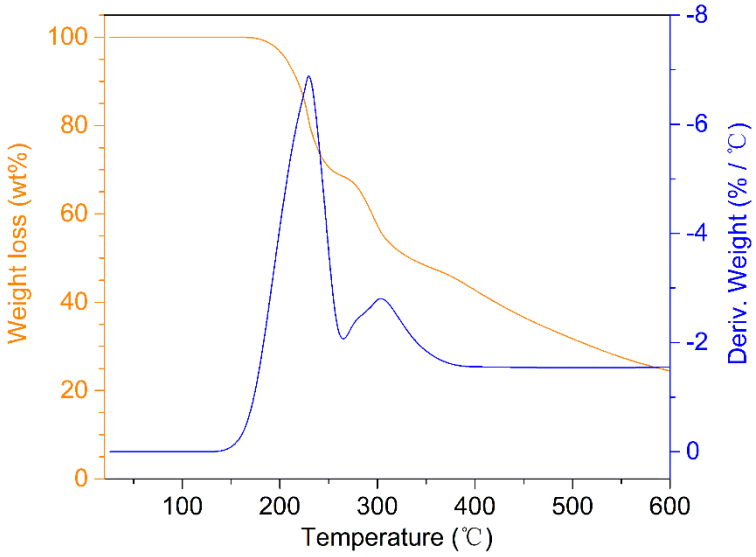

Figure S2. TGA curve of **1**.

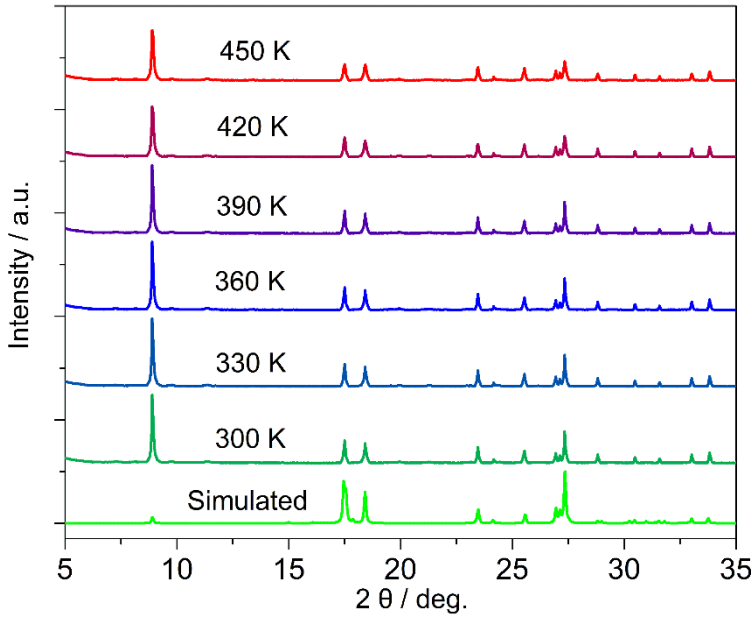

Figure S3. Variable-temperature PXRD patterns of **1**.

Table S1. Crystallographic data and structure refinement parameters for **1** at different measured temperature.

Complex	**1**		
Empirical formula	$C_{10}H_{16}CoO_{14}$		
Formula weight	419.16		
T / K	**100**	**300**	**400**
Crystal system	monoclinic		
Space group	*P*2/m		
a/Å	6.3747(5)	6.4912(5)	6.523(6)
b/Å	9.9302(8)	9.9169(8)	9.909(8)
c/Å	6.4394(6)	6.5380(6)	6.641(7)
α/°	90	90	90
β/°	114.467(2)	115.401(2)	115.98(4)
γ/°	90	90	90
Volume/Å^3	371.02(5)	380.18(6)	385.9(6)
Z	1		
ρ_{calc} g/cm^3	1.876	1.831	1.804
μ/mm^{-1}	1.237	1.207	1.190
F(000)	215.0		
2Θ range for data collection/°	4.102 to 56.076	4.108 to 55.03	4.11 to 54.92
Reflections collected	6878		
Independent reflections	912		
R_{int} / R_{sigma}	0.0339 / 0.0186		
Goodness-of-fit on F^2	1.140	1.126	1.115
R_1[a] / wR_2[b] ($I > 2\sigma(I)$)	0.0318 / 0.0855	0.0319 / 0.0875	0.0319 / 0.0887
R_1/ wR_2 (all data)	0.0331 / 0.0861	0.0331 / 0.0881	0.0332 / 0.0893
Max/min [e Å^{-3}]	0.73 / -0.33	0.74 / -0.29	0.75/-0.27

[a] $R_1 = \sum||F_o| - |F_c||/\sum|F_o|$ [b] $wR_2 = \{\sum[w(F_o^2 - F_c^2)2]/\sum[w(F_o^2)^2]\}^{1/2}$

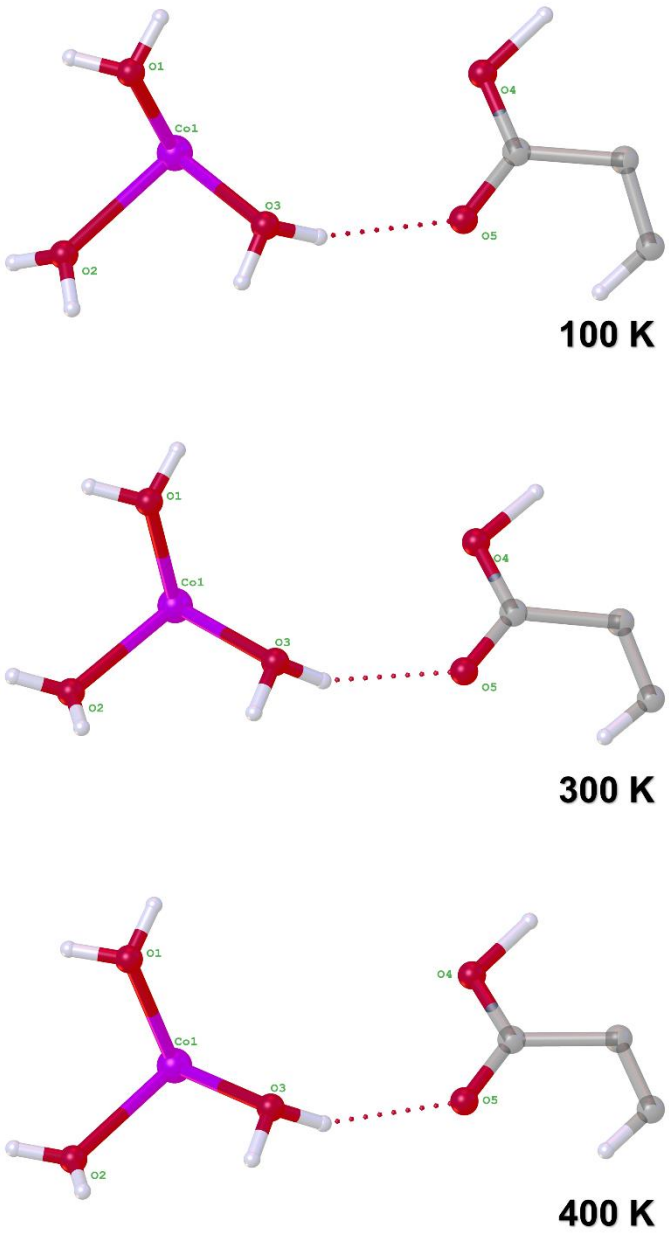

Figure S4. The asymmetric units of **1** measured at different temperatures.

Table S2. Selected bond lengths (Å) and angles [°] in **1**.

Parameter	**1**		
T / K	**100**	**300**	**400**
Co1-O1	2.096(3)	2.064(2)	2.020(3)
Co1-O1^{1}	2.096(3)	2.064(2)	2.020(3)
Co1-O2	2.112(3)	2.114(2)	2.120(2)
Co1-O2^{1}	2.112(3)	2.114(2)	2.120(2)
Co1-O3^{1}	2.047(3)	2.047(2)	2.036(2)
Co1-O3	2.047(3)	2.047(2)	2.036(2)
Co-O$_{averge}$	2.085	2.075	2.059
O1-Co1-O1^{1}	180.00(6)	180.00(18)	180.0
O1^{1}-Co1-O2^{1}	90.0	90.0	90.000(1)
O1^{1}-Co1-O2	90.0	90.0	90.000(1)
O1-Co1-O2^{1}	90.0	90.0	90.0
O1-Co1-O2	90.000(1)	90.000(1)	90.0
O2-Co1-O2^{1}	180.0	180.0	180.0
O3-Co1-O1	88.84(15)	90.79(12)	88.77(14)
O3^{1}-Co1-O1	91.16(15)	89.21(12)	91.23(14)
O3^{1}-Co1-O1^{1}	88.84(15)	90.79(12)	88.77(14)
O3-Co1-O1^{1}	91.16(15)	89.21(12)	91.23(14)
O3^{1}- Co1-O2	90.0	90.0	90.0
^{1}-X, 1-Y, 1-Z; ^{2}+X, 2-Y, + Z; ^{3}2-X, +Y, 2-Z			

Table S3. Continuous Shape Measure (CSM) analysis for six-coordinated Co(II) in **1**.

Compound, Metal center	T / K	CSM parameters* six-coordinated coordination sphere					Determined coordination geometry
		HP-6	PPY-6	OC-6	TPR-6	JPPY-6	
Co1	100	32.871	29.948	**0.052**	16.636	33.327	OC-6
	300	33.036	30.094	**0.022**	16.663	33.537	
	400	32.892	29.950	**0.024**	16.621	33.336	

*CSM[S2] parameters for six-coordinated complexes:

HP-6 - the parameter related to the hexagon (D_{6h})

PPY-6 - the parameter related to the pentagonal pyramid (C_{5v})

OC-6 - the parameter related to the octahedron (O_h)

TPR-6 - the parameter related to the trigonal prism (D_{3h})

JPPY-6 - the parameter related to the Johnson pentagonal pyramid (*C5v*)

Table S4. The possible hydrogen bonds in **1** at 100 K calculated by PLATON.

D-H...A	d(D- H)	d(H...A)	d(D...A)	＜(DHA)
O(1)-H(1A)...O(5)	0.86	2.09	2.7735	136
O(1)-H(1B)...O(5)	0.86	1.98	2.7735	152
O(2)-H(2A)...O(4)	0.84	2.08	2.7955	143
O(2)-H(2B)...O(4)	0.85	1.95	2.7955	177
O(3)-H(3A)...O(5)	0.85	2.01	2.7600	146
O(3)-H(3B)...O(5)	0.86	1.95	2.7600	157
O(7)-H(4)...O(5)	1.19	1.19	2.3817	174

Table S5. The possible hydrogen bonds in **1** at 300 K calculated by PLATON.

D-H...A	d(D- H)	d(H...A)	d(D...A)	＜(DHA)
O(1)-H(1A)...O(5)	0.86	2.00	2.7968	153
O(1)-H(1B)...O(5)	0.86	2.10	2.7968	137
O(2)-H(2A)...O(4)	0.85	2.02	2.8117	155
O(2)-H(2B)...O(4)	0.85	1.99	2.8117	161
O(3)-H(3A)...O(5)	0.86	1.96	2.7752	157
O(3)-H(3B)...O(5)	0.86	2.02	2.7752	146
O(7)-H(4)...O(5)	1.19	1.19	2.3785	175

Table S6. The possible hydrogen bonds in **1** at 400 K calculated by PLATON.

D-H...A	d(D- H)	d(H...A)	d(D...A)	＜(DHA)
O(1)-H(1A)...O(5)	0.87	2.02	2.8048	136
O(1)-H(1B)...O(5)	0.87	2.12	2.8048	152
O(2)-H(2A)...O(4)	0.85	2.02	2.8102	143
O(2)-H(2B)...O(4)	0.85	1.99	2.8102	177
O(3)-H(3A)...O(5)	0.86	1.96	2.7766	146
O(3)-H(3B)...O(5)	0.87	2.02	2.7766	157
O(4)-H(4)...O(4)	1.19	1.19	2.3760	174

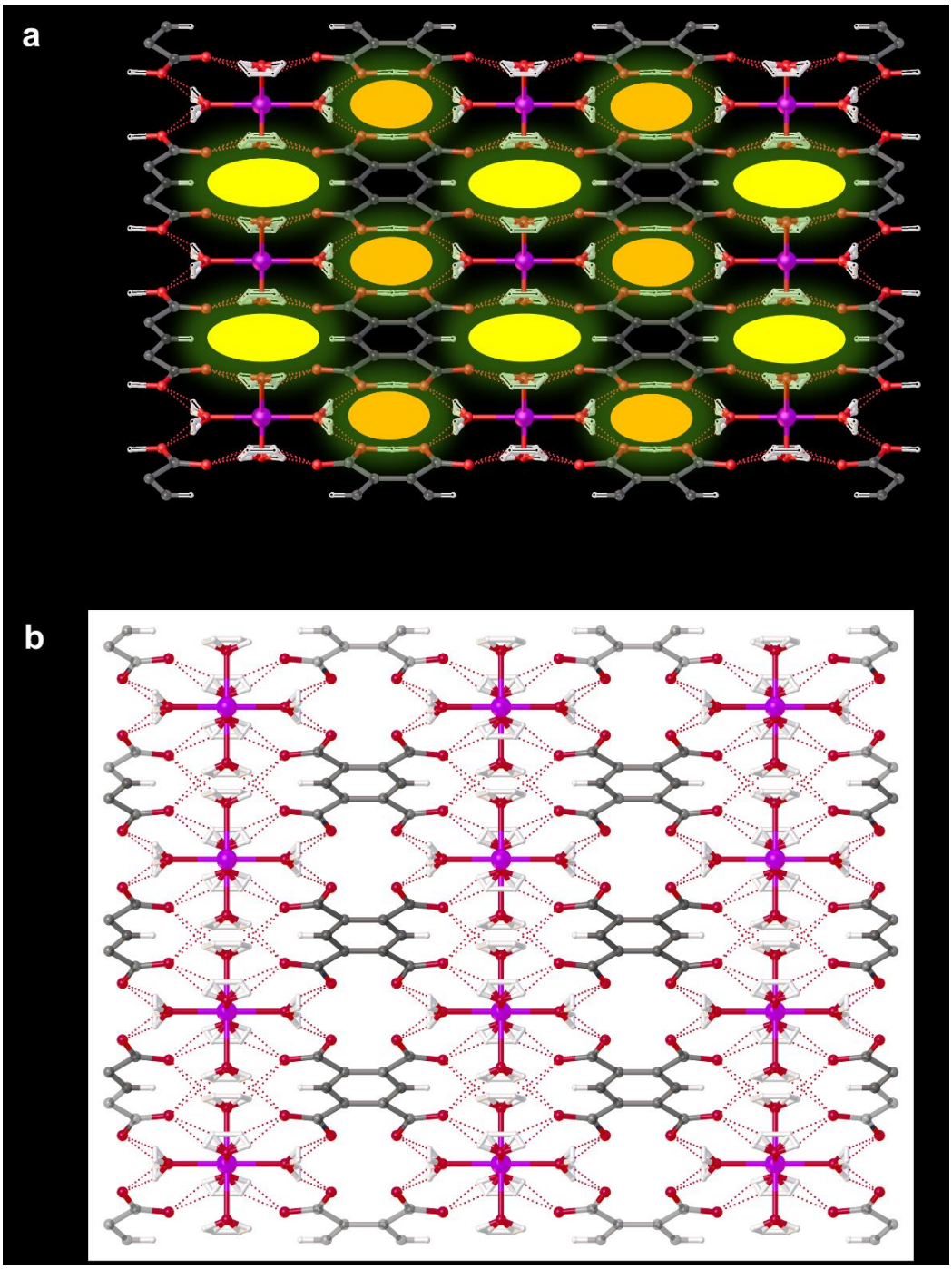

Figure S5. The open-pore structure and H-bonds networks in **1**.

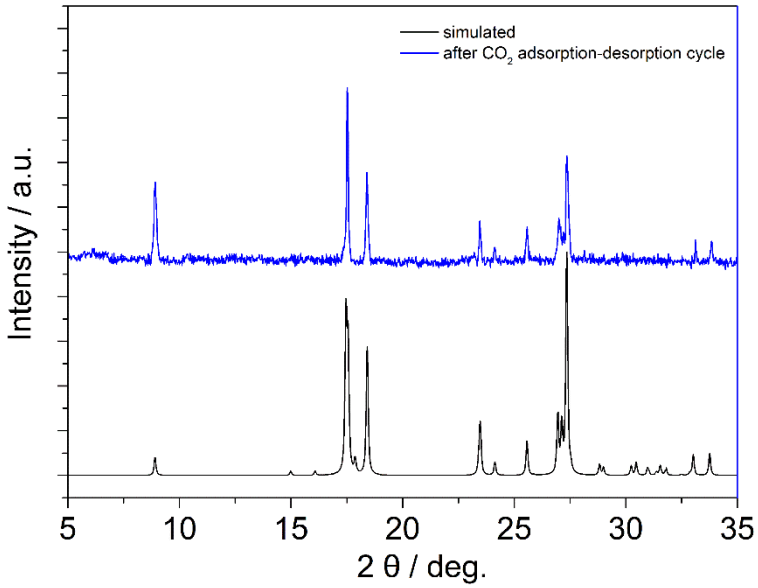

Figure S6. PXRD pattern of **1** measured after the CO2 adsorption/desorption experiment.

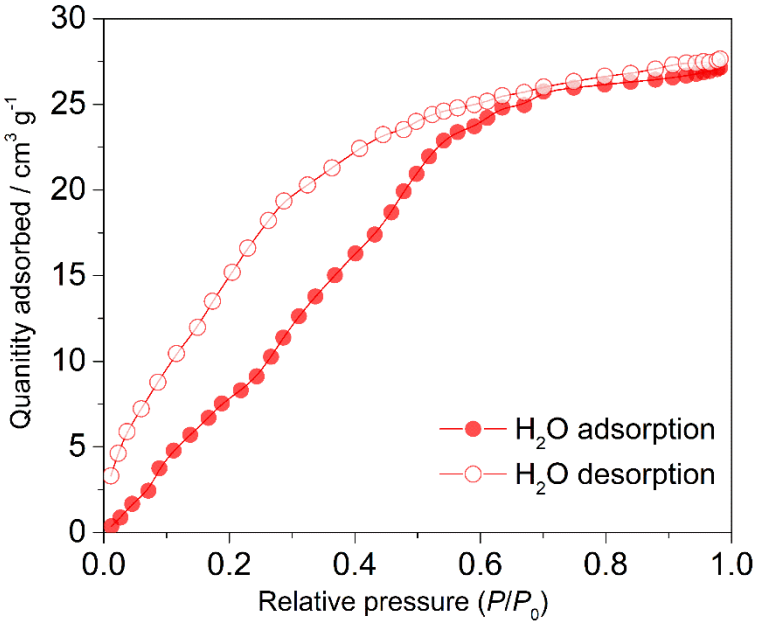

Figure S7. Water vapor adsorption/desorption isotherms of **1** measured at 25 °C.

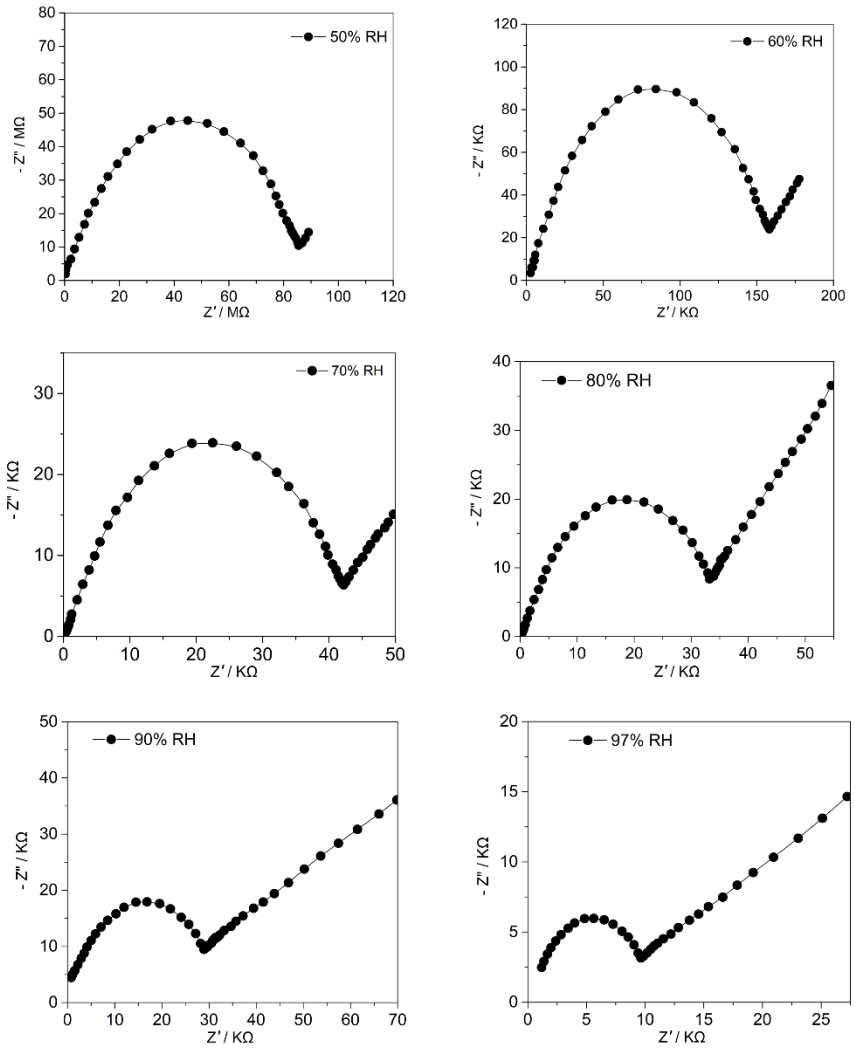

Figure S8. Nyquist plots of **1** at 313 K and different relative humidity of 70-97% RH.

Table S7. The conductivity of **1** extracted from impedance spectra gathered at 313 K under variable relative humidity.

RH%	σ / S cm^{-1}
40	4.1×10^{-8}
50	1.1×10^{-8}
60	3.5×10^{-7}
70	1.5×10^{-6}
80	6.7×10^{-5}
97	3.2×10^{-5}

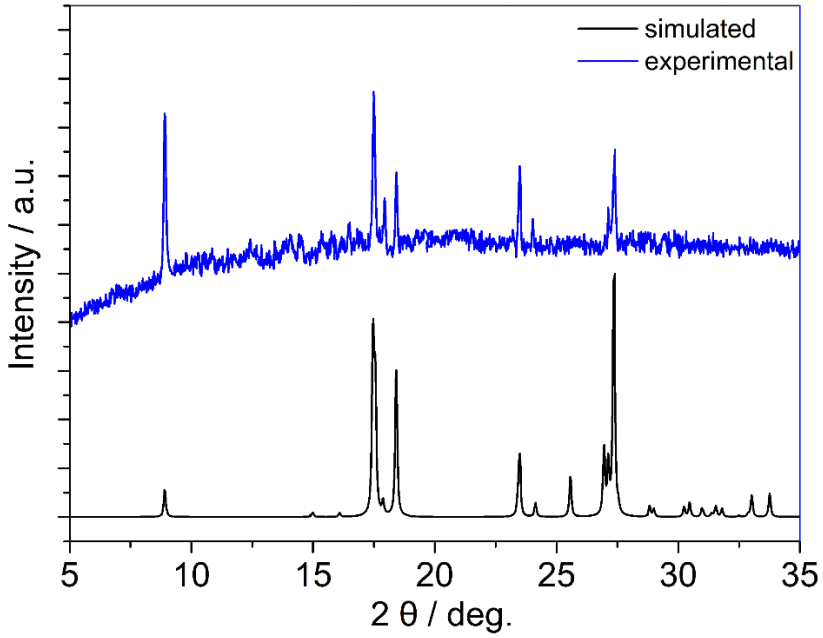

Figure S9. PXRD pattern of **1** after variable-humidity electrochemical test.

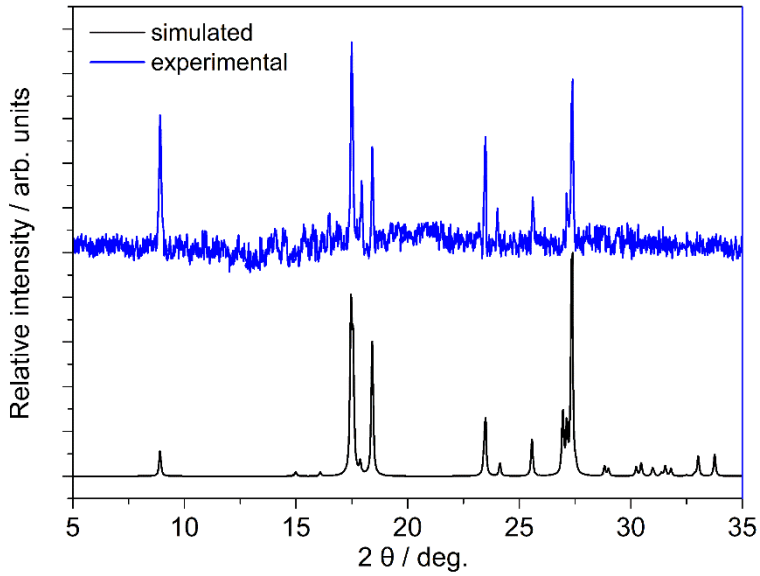

Figure S10. PXRD pattern of **1** after variable-temperature electrochemical test.

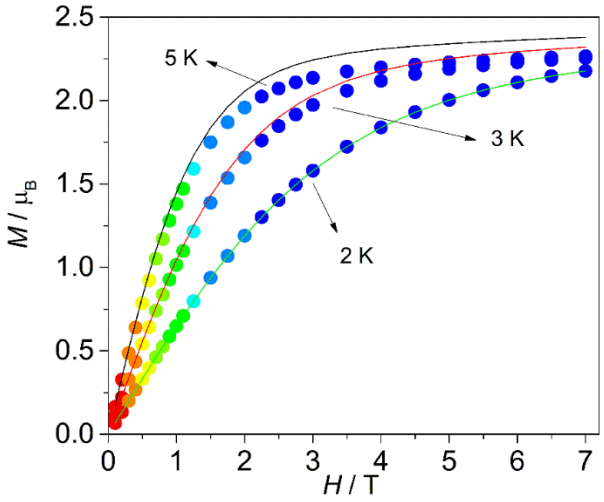

Figure S11. Variable-temperature magnetization curves of **1** measured at 2, 3, and 5 K. Solid lines represent the best fits.

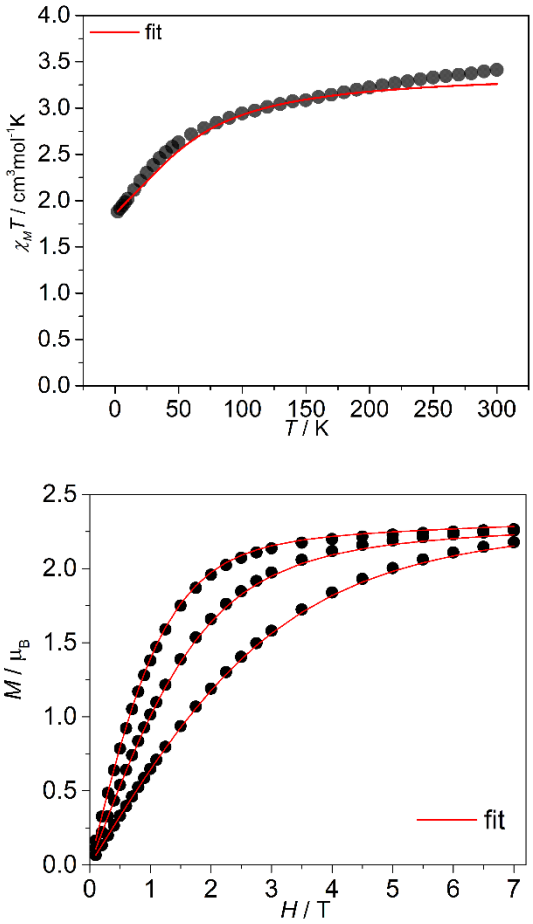

Figure S12. Variable-temperature magnetic susceptibility and magnetization curves of **1**. The red lines are the simulation by the Figgis–Griffith Hamiltonian as described in the main text.

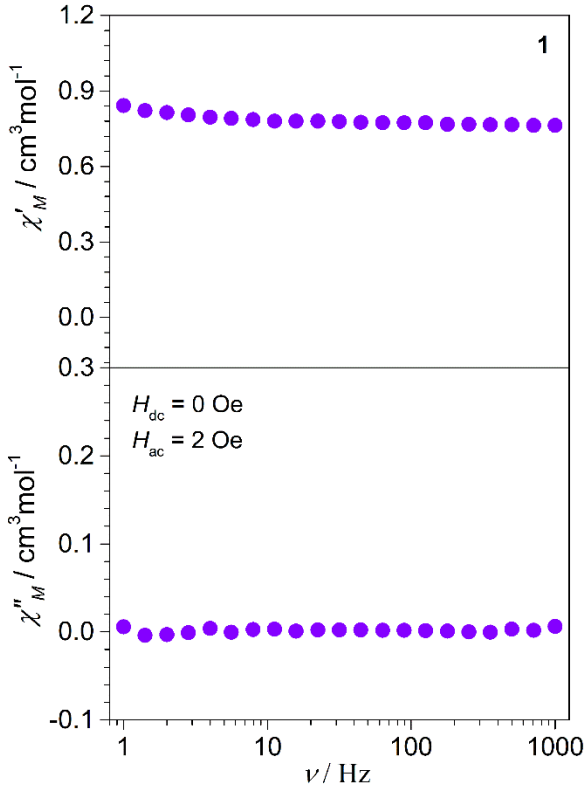

Figure S13. Frequency dependence of the ac susceptibility measured under zero dc field at 2.0 K for **1**.

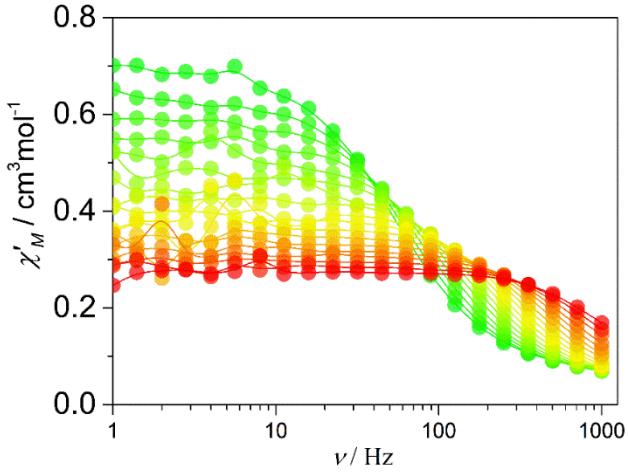

Figure S14. Frequency dependence of the in-phase (χ') ac susceptibility measured under 1 kOe dc field in the temperature range of 2-6.2 K for **1**.

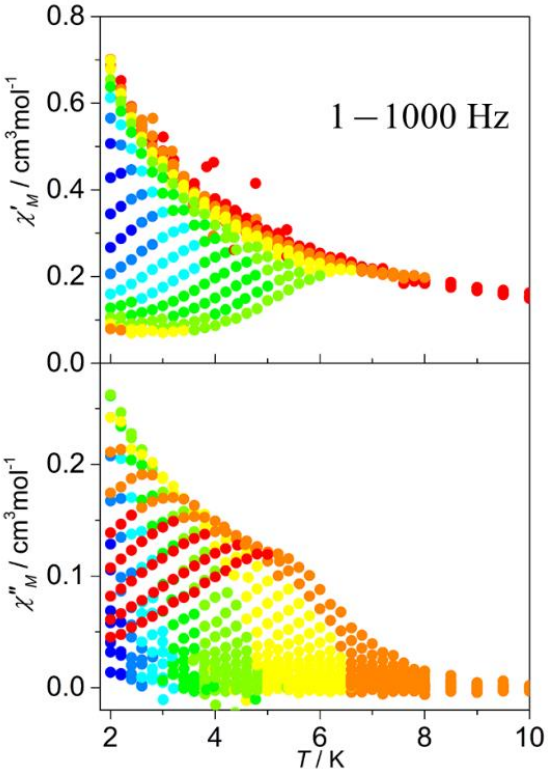

Figure S15. Temperature dependence of the in-phase (χ') and out-of-phase (χ'') ac susceptibilities measured under 1 kOe dc field in the temperature range of 2-10 K for **1**.

Table S8. Relaxation fitting parameters from the least-square fitting of the Cole-Cole plots of **1** under 1 kOe dc filed according to the generalized Debye model.

T / K	τ / s	χ_S / $cm^3mol^{-1}K$	χ_T / $cm^3mol^{-1}K$	α
1.99994	0.00294	0.0675	0.70789	0.11161
2.19994	0.00237	0.06286	0.64494	0.10296
2.39996	0.00192	0.06023	0.59712	0.08995
2.59975	0.00158	0.05702	0.55546	0.08725
2.80137	0.00133	0.05247	0.52613	0.0958
2.99902	0.00109	0.05255	0.48247	0.06969
3.19759	9.22309E-4	0.04996	0.45807	0.07028
3.4001	7.71706E-4	0.04967	0.42895	0.05592
3.6005	6.46946E-4	0.04697	0.40332	0.05016
3.79965	5.53468E-4	0.0459	0.38583	0.04693
3.99794	4.75312E-4	0.04228	0.37494	0.06241
4.20018	4.02112E-4	0.04391	0.35252	0.04402
4.40041	3.3633E-4	0.03915	0.3386	0.0496
4.60088	2.82108E-4	0.03747	0.32483	0.05174
4.79827	2.37291E-4	0.03251	0.31464	0.05992
5.00096	1.96874E-4	0.03257	0.30075	0.05536
5.20301	1.63246E-4	0.02984	0.2874	0.04259

References

S1) SAINT Software Users Guide, version 7.0; Bruker Analytical X-Ray Systems: Madison, WI, 1999.

S2) G. M. Sheldrick, SADABS, version 2.03; Bruker Analytical X-Ray Systems, Madison, WI, 2000.

S3) G. M. Sheldrick, SHELXTL, Version 6.14, Bruker AXS, Inc.; Madison, WI 2000-2003.

S4) Dolomanov, O. V.; Bourhis, L. J.; Gildea, R. J.; Howard, J. A. K.; Puschmann, H. OLEX2: A Complete Structure Solution, Refinement and Analysis Program. J. Appl. Crystallogr., 2009, 42, 339−341.